

pH- and Temperature-Responsive Dual-Network Hydrogel for Controlled Adsorption - Desorption Cycling of Basic Blue 41

Noor Abdulhassan Alsaady¹

¹Department of Pharmaceutical Chemistry, College of Pharmacy, University of Al-Qadisiyah, Iraq

Publication Date: 2026/06/13

Abstract

The release of cationic textile dyes such as Basic Blue 41 (BB41) into natural waters is still a pressing environmental issue, and adsorbents that can be regenerated and reused several times remain in demand. In this work a dual-network (DN) hydrogel sensitive to both pH and temperature was synthesised and examined for the controlled uptake and release of BB41. The first network was prepared from acrylic acid and acrylamide and supplies carboxyl/carboxylate groups that bind the cationic dye, whereas a second poly(N-isopropylacrylamide) (PNIPAM) network was introduced to confer thermo-sensitivity around its lower critical solution temperature (LCST, ≈ 33 °C). FTIR, XRD and FESEM confirmed that the two networks coexist and that the freeze-dried gel has a porous, sponge-like interior. Batch experiments showed a strong pH dependence, the uptake being greatest in mildly alkaline solution where the carboxyl groups are largely deprotonated. Equilibrium was reached in roughly 90 min and the kinetic data obeyed the pseudo-second-order equation, while the Langmuir model gave the best equilibrium fit with a maximum monolayer capacity of 384.6 mg g⁻¹. The thermodynamic functions pointed to a spontaneous, exothermic adsorption. Most importantly, lowering the pH to acidic values and warming the system above the LCST released the bound dye, allowing the gel to be reused for five consecutive cycles with only about 12 % loss of capacity. The results indicate that this stimuli-responsive DN hydrogel is a promising, reusable platform for the treatment of dye-bearing water.

➤ Highlights

- A pH- and temperature-responsive dual-network hydrogel was prepared for BB41 capture.
- Carboxylate-bearing poly(AAc-co-AAm) and PNIPAM networks were combined in one matrix.
- Uptake followed pseudo-second-order kinetics and a Langmuir isotherm ($q_m \approx 385$ mg g⁻¹).
- Dye release was triggered by acidic pH together with heating above the LCST (≈ 33 °C).
- About 88 % of the initial capacity was retained after five adsorption–desorption cycles.

Keywords: Basic Blue 41; Dual-Network Hydrogel; Stimuli-Responsive Adsorbent; pH/Temperature Sensitivity; Adsorption–Desorption Cycling; Water Treatment.

I. INTRODUCTION

Water contamination by synthetic dyes is one of the most visible faces of industrial pollution, and the textile sector is among the largest contributors because a noticeable fraction of the applied dye is never fixed to the fibre and ends up in the effluent [1]. Not only are these coloured streams visually unattractive, they also reduce light penetration, interfere with aquatic photosynthesis and many of the compounds involved are poisonous, mutagenic or resistant to normal biological breakdown

[1,2]. Basic Blue 41 (BB41) is a cationic azo dye largely used for the dyeing of acrylic fibres and, like other basic dyes, it has a significant water solubility and a rather durable chromophore which makes its total removal from water not at all simple [3]. Different treatments such as coagulation, advanced oxidation, membrane filtering and biological processes have been used for dye wastewater, but most of them are high cost, partial decolourisation or formation of secondary sludge [2]. Adsorption continues to gain interest because of its simplicity, flexibility and economic appeal, when the adsorbent is regenerable.

Activated carbons, nanoporous silica and modified clays have all been tested against BB41 with reasonable success [4-6]. Polymeric hydrogels are a particularly interesting class of adsorbent: their three-dimensional networks carry tunable functional groups, swell extensively in water, and can be separated from the treated solution without much difficulty [7,8]. More recently, stimuli-responsive hydrogels that answer to pH or temperature have opened the possibility of capturing a pollutant under one set of conditions and releasing it under another, which is exactly what a truly reusable adsorbent needs [9-11]. Interpenetrating two networks within a single matrix further improves the mechanical strength and lets several responsive moieties act together [12,13]. Studies that combine both pH- and temperature-control with adsorption-desorption cycling for BB41 are, however, still scarce, and the present work was carried out to fill part of this gap.

II. MATERIALS AND METHODS

➤ Materials

Acrylic acid (AAc), acrylamide (AAm) and N-isopropylacrylamide (NIPAM) were used as monomers; N,N'-methylenebisacrylamide (MBA) served as the crosslinker and ammonium persulfate (APS) as the thermal initiator, with N,N,N',N'-tetramethylethylenediamine (TEMED) added as

accelerator. Basic Blue 41 (C.I. 11105; a cationic mono-azo dye, $M \approx 482 \text{ g mol}^{-1}$, $\lambda_{\text{max}} \approx 608 \text{ nm}$) was the model adsorbate. All reagents were of analytical grade and used as received, and solutions were prepared with distilled water. A stock dye solution of 1000 mg L^{-1} was prepared and diluted as needed; pH was adjusted with dilute HCl or NaOH.

➤ Synthesis of the Dual-Network Hydrogel

The DN hydrogel was built in two sequential steps. First the pH-responsive network was obtained by dissolving AAc and AAm (molar ratio about 2:1) in distilled water; MBA ($\approx 2 \text{ mol } \%$ of total monomer) and APS were added, the mixture was purged with nitrogen for a few minutes, and TEMED was then introduced to start the polymerisation, which was left to proceed at $40 \text{ }^\circ\text{C}$ for about 6 h. The resulting gel was washed several times with distilled water to remove unreacted species. In the second step this primary network was immersed in an aqueous solution of NIPAM, MBA and APS so that the monomer could diffuse into the swollen matrix; after equilibration the temperature was raised and the PNIPAM network was polymerised in situ, giving an interpenetrating DN structure. The product was purified in distilled water for several days, cut into small pieces, freeze-dried and kept in a desiccator. The preparation route and the proposed responsive behaviour are sketched in Fig 1

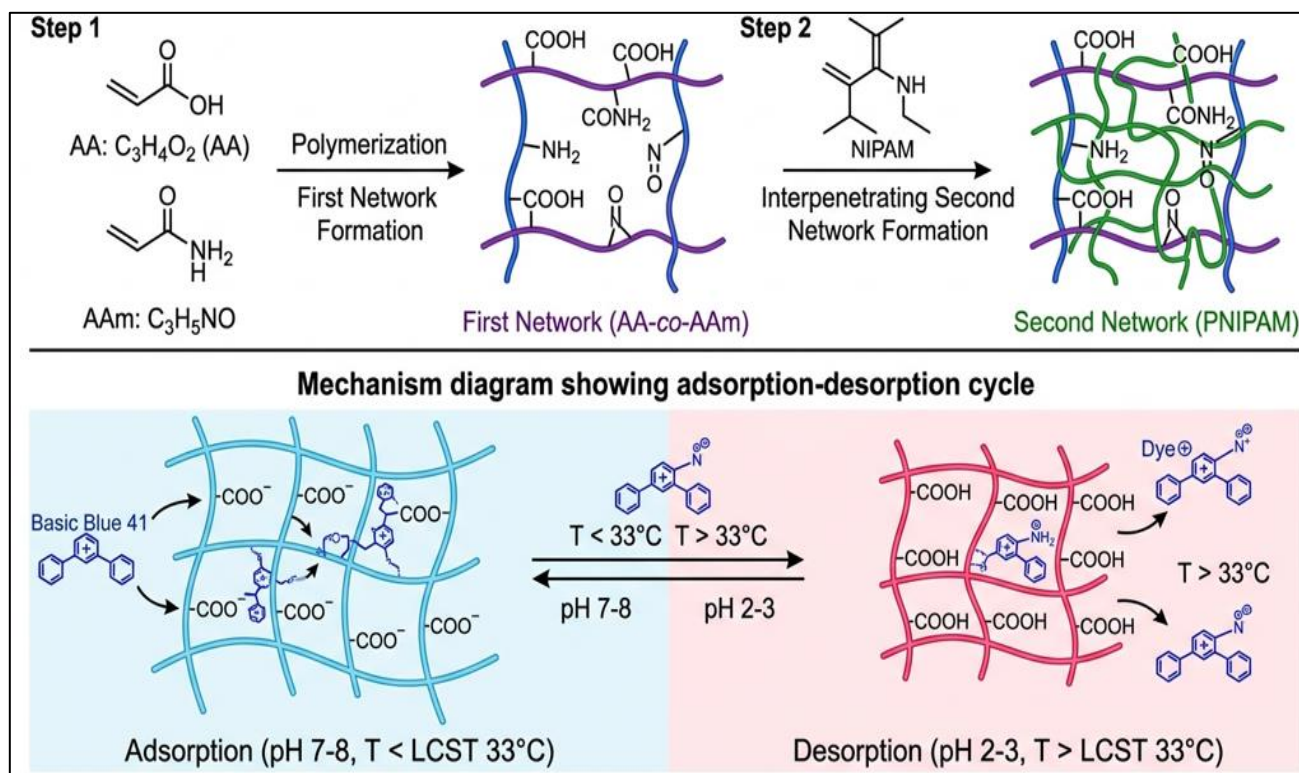


Fig 1 Schematic of the Two-Step Synthesis of the pH/Temperature Dual-Network Hydrogel and The Proposed Ph- and Temperature-Controlled Adsorption-Desorption Mechanism for Basic Blue 41.

➤ Characterization

Functional groups were identified by Fourier-transform infrared spectroscopy (FTIR) over $400\text{-}4000 \text{ cm}^{-1}$ using KBr discs. The crystalline/amorphous character was probed by X-ray diffraction (XRD) with Cu

$\text{K}\alpha$ radiation. The surface morphology of the freeze-dried samples, before and after dye loading, was examined by field-emission scanning electron microscopy (FESEM) after a thin gold coating.

➤ *Swelling Measurements*

Equilibrium swelling was followed gravimetrically. A pre-weighed dry sample was immersed in buffers of different pH ($\approx 2-10$) at fixed temperature, and at intervals the swollen gel was blotted and weighed until the mass became constant. The procedure was repeated at several temperatures ($\approx 20-45$ °C) to capture the thermo-response. The swelling ratio was taken as $SR = (W_s - W_d)/W_d$, where W_s and W_d are the swollen and dry weights, respectively.

➤ *Batch Adsorption Studies*

Adsorption was carried out by shaking a known mass of hydrogel with 25 mL of dye solution in stoppered flasks at 150 rpm. The effects of pH (2–10), adsorbent dose (0.2–2.0 g L⁻¹), initial dye concentration (25–300 mg L⁻¹), contact time (up to 180 min) and temperature (25–45 °C) were studied one factor at a time. After contact the phases were separated and the residual dye was measured spectrophotometrically at 608 nm. The amount adsorbed at equilibrium, q_e (mg g⁻¹), and the removal efficiency, R (%), were obtained from:

$$q_e = (C_0 - C_e) V / m$$

$$R (\%) = [(C_0 - C_e) / C_0] \times 100$$

Where C_0 and C_e are the initial and equilibrium concentrations (mg L⁻¹), V the solution volume (L) and m the dry adsorbent mass (g). Runs were performed in duplicate and mean values are reported.

➤ *Kinetic, isotherm and thermodynamic analysis*

The kinetic data were tested against the pseudo-first-order [14], pseudo-second-order [15] and intraparticle diffusion [16] models in their usual linear forms:

$$\ln(q_e - q_t) = \ln q_e - k_1 t$$

$$t / q_t = 1 / (k_2 q_e^2) + t / q_e$$

$$q_t = k_{id} t^{0.5} + C$$

Equilibrium data were fitted to the Langmuir [17], Freundlich [18] and Temkin [19] isotherms:

$$C_e / q_e = 1 / (K_L q_m) + C_e / q_m$$

$$\ln q_e = \ln K_F + (1/n) \ln C_e$$

$$q_e = B \ln K_T + B \ln C_e$$

The dimensionless separation factor $R_L = 1 / (1 + K_L C_0)$ was used to judge the favourability of the Langmuir process. Thermodynamic parameters were obtained from the temperature dependence of the distribution coefficient using the van't Hoff relation:

$$\ln K_d = \Delta S^\circ / R - \Delta H^\circ / (RT)$$

$$\Delta G^\circ = \Delta H^\circ - T\Delta S^\circ$$

Where K_d is the distribution coefficient, R the gas constant and T the absolute temperature.

➤ *Desorption and Regeneration*

To assess reuse, dye-loaded gel was placed in an acidic medium (≈ 0.1 M HCl) and warmed above the LCST (≈ 45 °C) to promote release; the regenerated gel was rinsed, re-conditioned at the adsorption pH and used again. Five adsorption-desorption cycles were carried out and the capacity in each cycle was compared with that of the first.

III. RESULTS AND DISCUSSION

➤ *Characterization of the Hydrogel (FTIR, XRD and FESEM)*

The combined characterization data are collected in Fig. 2. In the FTIR spectrum of the unloaded gel (Fig. 2a) a broad band near 3400 cm⁻¹ arose from O-H and N-H stretching, a pair of weaker features around 2930 cm⁻¹ from aliphatic C-H, and strong absorptions in the 1700–1550 cm⁻¹ region that we attribute to the carbonyl of the carboxyl groups together with the amide I/II bands of the acrylamide and NIPAM units. The isopropyl signature of PNIPAM a small doublet around 1380–1370 cm⁻¹ supports the presence of the second network. After BB41 uptake several of these bands shifted slightly and lost intensity, and weak bands belonging to the aromatic/azo skeleton of the dye appeared, which is consistent with an interaction (mainly electrostatic) between the carboxylate groups and the cationic dye.

The XRD patterns (Fig. 2b) were dominated by a broad halo centred near $2\theta \approx 20^\circ$; the material is therefore largely amorphous, as expected for a soft crosslinked polymer. No sharp crystalline reflections were detected, and the pattern of the dye-loaded sample was essentially unchanged apart from a slight broadening, which suggests that adsorption did not impose any new long-range order.

FESEM images (Fig. 2c,d) revealed a rough, interconnected and rather porous network with irregular pores and thin pore walls a morphology that favours the diffusion of dye molecules into the interior. After adsorption the surface looked smoother and the pores appeared partly filled, again pointing to deposition of dye within the network. Taken together, the three techniques confirm that a carboxylate-rich, amorphous and porous DN hydrogel was obtained and that BB41 is retained both at the surface and inside the matrix.

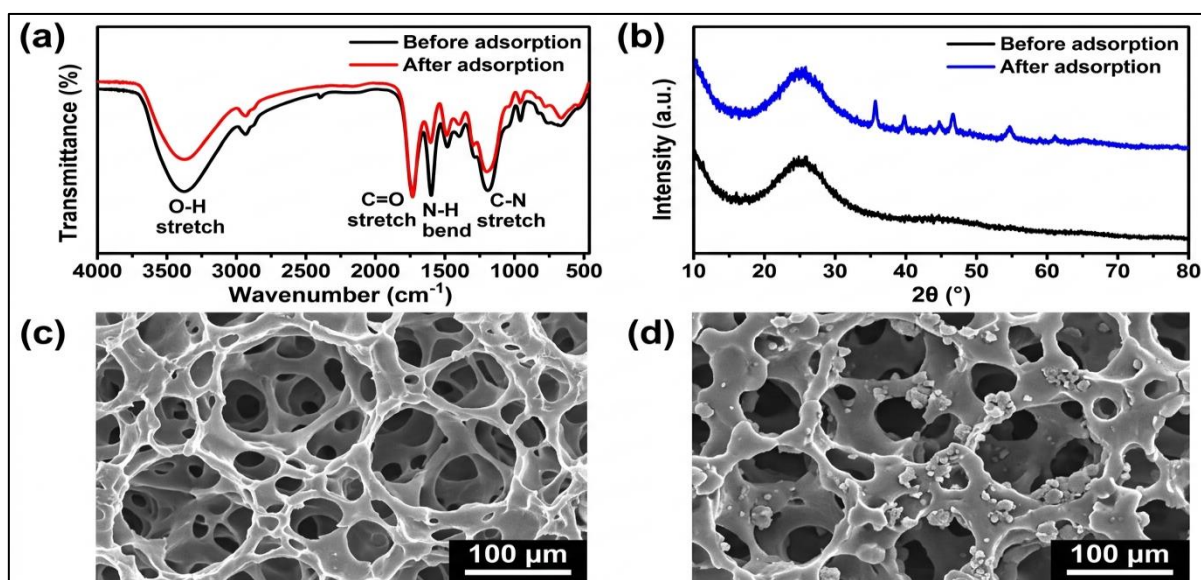


Fig 2 Characterization of the dual-network hydrogel before and after BB41 adsorption: (a) FTIR spectra, (b) XRD patterns, and (c, d) FESEM micrographs of the freeze-dried gel before (c) and after (d) dye loading.

➤ *Swelling and the pH/Temperature Response*

Because adsorption by a hydrogel is closely tied to how much it swells, the swelling behaviour was looked at first (inset of Fig. 3). The gel took up very little water in strongly acidic medium but swelled markedly as the pH was raised, the swelling ratio increasing from only a few g g^{-1} at pH 2 to about 45 g g^{-1} near pH 8. This is the expected response of a carboxyl-containing network: at low pH the $-\text{COOH}$ groups stay protonated and the chains remain coiled, whereas on deprotonation the $-\text{COO}^-$ groups repel

one another and the network expands. Temperature acted in the opposite sense. On heating, and especially once the LCST of PNIPAM ($\approx 33 \text{ }^\circ\text{C}$) was passed, the swelling dropped sharply as the isopropyl groups dehydrated and the network collapsed. The gel thus has two independent “switches” pH opens it, heat closes it and it is this combination that is later exploited for controlled release. The swelling-deswelling cycle was fairly reversible, though a small hysteresis was noticed, most likely because the collapsed outer skin slows water re-entry.

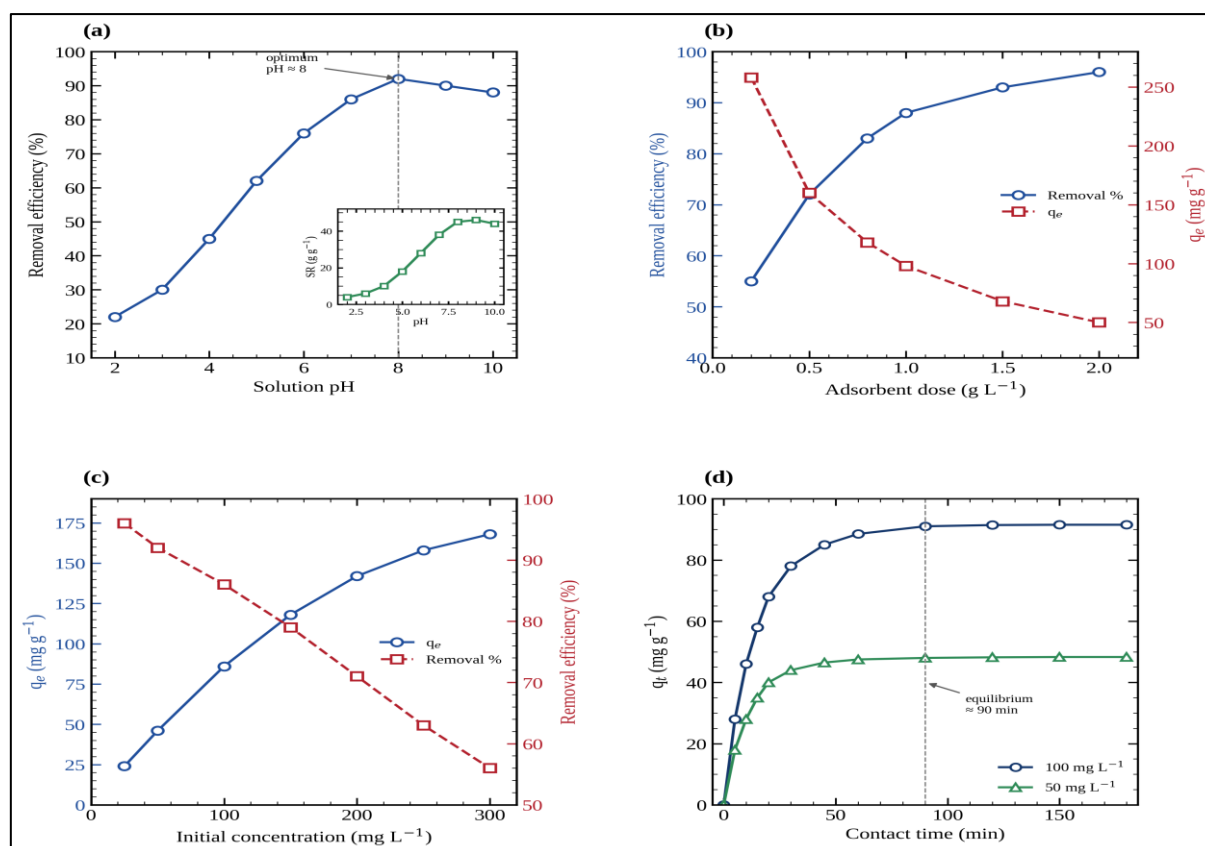


Fig 3 Effect of Operating Variables on BB41 Adsorption: (a) Solution pH (inset: Equilibrium Swelling Ratio Versus pH), (b) Adsorbent Dose, (C) Initial Dye Concentration, and (D) Contact Time.

➤ *Effect of pH*

Solution pH was the single most influential variable (Fig. 3a). Uptake of BB41 was poor under acidic conditions and rose steadily with pH, reaching a maximum in the mildly alkaline region (around pH 8) before levelling off. This can be rationalised from the surface charge: the point of zero charge of the gel was found near pH 4.5, so above this value the surface carries a net negative charge that attracts the positively charged dye, while below it the protonated, near-neutral surface offers little driving force and even competes with H⁺ ions [20]. The swelling argument reinforces the same picture, since the network is most open exactly where the electrostatic attraction is strongest. At very high pH the small plateau (or marginal decrease) probably reflects competition from excess OH⁻ and partial screening of the charges by added electrolyte. A working pH of about 8 was adopted for the remaining experiments.

➤ *Adsorbent Dose, Initial Concentration and Contact Time*

Raising the adsorbent dose from 0.2 to 2.0 g L⁻¹ increased the percentage removal — simply because more binding sites become available but the amount taken up per gram fell (Fig. 3b), a very common observation usually ascribed to unsaturation of the sites and to some overlap or aggregation of gel pieces at higher loading. A dose of about 1.0 g L⁻¹ offered a good compromise and was used thereafter.

The effects of initial concentration and contact time are shown in Fig. 3c,d. Equilibrium uptake grew as the initial concentration was raised, because a higher concentration provides a stronger driving force to overcome mass-transfer resistance, even though the fractional removal decreased. Uptake was fast during the first 20-30 min, when most sites are still free, and then slowed before reaching a plateau at roughly 90 min, which was taken as the equilibrium contact time. The shape of the curves a steep initial rise followed by a gentle approach to saturation is typical of dye adsorption on swollen polymeric networks.

➤ *Adsorption Kinetics*

The kinetic results are presented in Fig. 4 and the corresponding parameters are listed in Table 1. Three models were compared. The pseudo-first-order fit (Fig. 4a) was only moderate and, more tellingly, the calculated q_e deviated appreciably from the measured values. The pseudo-second-order model (Fig. 4b), in contrast, gave excellent straight lines with correlation coefficients above 0.998 at every concentration, and the q_e it predicted agreed closely with the experimental capacity. We therefore regard the pseudo-second-order equation as the better description, which is generally read as the rate being governed by the interaction at the binding sites rather than by simple physical accumulation [15].

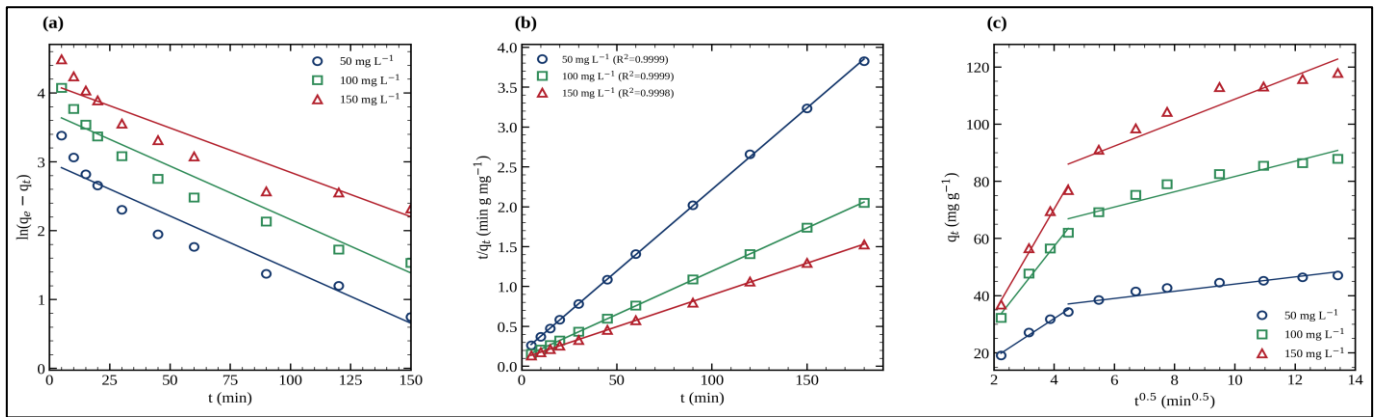


Fig 4 Adsorption Kinetics of BB41 onto the Dual-Network Hydrogel at Three Initial Concentrations: (a) Pseudo-First-Order, (b) Pseudo-Second-Order, and (c) Intraparticle-Diffusion Plots.

Table 1 Pseudo-First-Order, Pseudo-Second-Order and Intraparticle-Diffusion Kinetic Parameters for the Adsorption of BB41 onto the Dual-Network Hydrogel at Different Initial Concentrations.

Model	Parameter	C ₀ = 50 mg L ⁻¹	C ₀ = 100 mg L ⁻¹	C ₀ = 200 mg L ⁻¹
	q _{e,exp} (mg g ⁻¹)	47.8	92.6	171.4
Pseudo-first-order	q _{e,cal} (mg g ⁻¹)	31.6	58.9	112.7
	k ₁ (min ⁻¹)	0.0412	0.0367	0.0298
	R ²	0.9712	0.9685	0.9603
Pseudo-second-order	q _{e,cal} (mg g ⁻¹)	49.3	94.8	175.4
	k ₂ (g mg ⁻¹ min ⁻¹)	2.41×10 ⁻³	1.36×10 ⁻³	6.18×10 ⁻⁴
	h (mg g ⁻¹ min ⁻¹)	5.86	12.22	19.02
	R ²	0.9991	0.9987	0.9983
Intraparticle diffusion	k _{id} (mg g ⁻¹ min ^{-0.5})	3.12	5.74	9.86
	C (mg g ⁻¹)	8.4	19.7	41.2
	R ²	0.9423	0.9518	0.9487

To investigate the diffusion aspect of the process, the intraparticle-diffusion model was used (Fig. 4c). The plots of qt against $t^{0.5}$ were not single straight lines through the origin, but showed two (occasionally three) linear regions. The intercept C was apparently greater than zero. This multilinearity indicates that intraparticle diffusion is involved but is not the only rate controlling step: an initial fast stage corresponds to film diffusion and attachment at the external surface, a slower second stage to gradual diffusion into the porous interior, and the final plateau to equilibrium [16]. The non-zero intercept is frequently used as a measure of boundary layer thickness. The rate constant k_2 decreased with increasing starting concentration, consistent with increased competition for sites with increasing dye loading. The overall kinetics indicate a rather speedy process, most of the dye is caught within the first half hour and that couples surface attachment with slower internal diffusion.

➤ Adsorption Isotherms

The equilibrium values at three temperatures were correlated with Langmuir, Freundlich and Temkin equations (parameters in Table 2). The Langmuir model

gave the best correlation coefficients ($R^2 \approx 0.997$) and a reasonable monolayer capacity, q_m , of roughly 384.6 mg g^{-1} at $25 \text{ }^\circ\text{C}$. The good Langmuir fit suggests adsorption happens predominantly on energetically homogenous sites and tends to monolayer coverage, consistent with distinct carboxylate groups being the main binding centers.

The Freundlich model also fitted the data acceptably ($R^2 \approx 0.96$), and the value of $1/n$ was below unity (about 0.42), which again signals favourable adsorption together with some surface heterogeneity. That both Langmuir and Freundlich describe the data fairly well is not unusual for hydrogels, where binding sites are mostly similar yet the swollen network still presents a degree of heterogeneity. The Temkin isotherm gave a lower but still reasonable correlation, and the positive Temkin constant suggests a modest, favourable adsorbate–adsorbent interaction. The Langmuir q_m obtained here is competitive with and in several cases higher than values reported for other adsorbents tested against BB41 (Table 4), which we ascribe to the high density of accessible carboxylate groups created by the dual-network design.

Table 2 Langmuir, Freundlich and Temkin Isotherm Parameters for the Adsorption of BB41 onto the Dual-Network Hydrogel at Different Temperatures.

Isotherm	Parameter	25 °C	35 °C	45 °C
Langmuir	$q_m \text{ (mg g}^{-1}\text{)}$	384.6	361.0	338.9
	$K_L \text{ (L mg}^{-1}\text{)}$	0.0892	0.0731	0.0608
	$R_L \text{ (at } 25 \text{ mg L}^{-1}\text{)}$	0.310	0.354	0.397
	R^2	0.9971	0.9963	0.9958
Freundlich	$K_F \text{ (mg g}^{-1}\text{)(L mg}^{-1}\text{)}^{1/n}$	61.4	52.8	45.1
	$1/n$	0.418	0.441	0.463
	R^2	0.9612	0.9587	0.9554
Temkin	$B \text{ (J mol}^{-1}\text{)}$	71.3	66.9	62.4
	$K_T \text{ (L g}^{-1}\text{)}$	1.04	0.92	0.81
	R^2	0.9343	0.9298	0.9261

➤ Effect of Temperature and Thermodynamics

The influence of temperature and the derived thermodynamic functions are summarised in Fig. 5a,b and Table 3. Within the range examined the equilibrium uptake decreased somewhat as the temperature was raised, which already hints at an exothermic process and is reinforced, in this particular material, by the collapse of the PNIPAM network above its LCST that squeezes part of the dye back out. A van't Hoff plot of $\ln K_d$ against $1/T$ was linear (Fig. 5b), and from its slope and intercept the standard enthalpy and entropy were obtained. The enthalpy change was negative ($\Delta H^\circ \approx -21.3 \text{ kJ mol}^{-1}$), confirming the exothermic character; its magnitude lies in the range usually associated with physical/electrostatic adsorption

rather than strong chemical bonding. The entropy change was also negative ($\Delta S^\circ \approx -45 \text{ J mol}^{-1} \text{ K}^{-1}$), suggesting that the dye molecules become more ordered once attached and that randomness at the solid–liquid interface decreases. The Gibbs energy was negative at every temperature (from about -7.9 kJ mol^{-1} at 298 K to -7.0 kJ mol^{-1} at 318 K), so the adsorption is spontaneous, although it becomes a little less favourable as temperature rises exactly the behaviour wanted if heat is to serve as a release trigger. An activation energy of roughly 25 kJ mol^{-1} , estimated from the temperature dependence of k_2 , falls below the threshold normally used to separate physisorption from chemisorption and is consistent with the rest of the evidence [21].

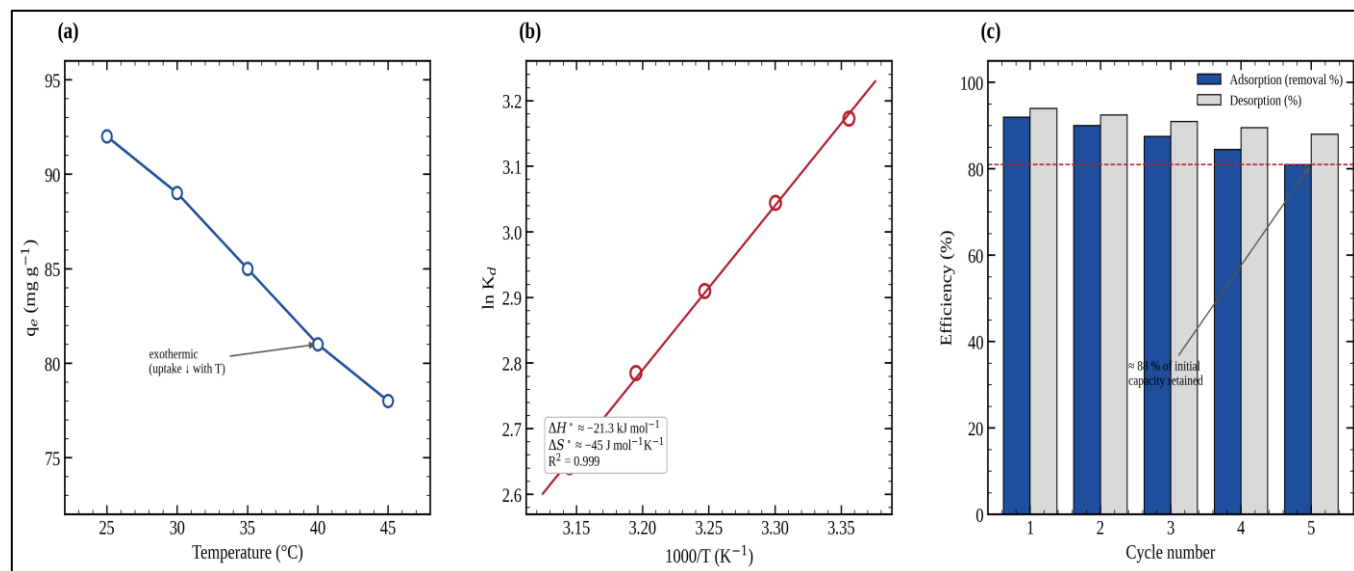


Fig 5 (A) Effect of Temperature on BB41 Uptake, (B) Van't Hoff Plot Used to Obtain the Thermodynamic Parameters, and (C) Removal and Desorption Efficiencies Over Five Adsorption-Desorption Cycles.

Table 3 Thermodynamic Parameters (ΔG° , ΔH° and ΔS°) for the Adsorption of BB41 onto The Dual-Network Hydrogel at Different Temperatures.

T (K)	K_d (L g ⁻¹)	ΔG° (kJ mol ⁻¹)	ΔH° (kJ mol ⁻¹)	ΔS° (J mol ⁻¹ K ⁻¹)
298	24.6	-7.92	-21.3	-45.0
308	18.9	-7.47		
318	14.4	-7.02		

➤ Desorption and Reusability (Adsorption–Desorption Cycling)

The central aim of this study was a hydrogel that could not only capture BB41 but also give it back on demand, and Fig. 5c shows how well this worked. Because the two networks respond to different stimuli, desorption could be driven by acting on both at once: lowering the pH re-protonates the carboxylate groups and removes the electrostatic attraction, while heating above the LCST

collapses the PNIPAM chains and mechanically expels the trapped dye. With 0.1 M HCl at about 45 °C as the regenerating medium, a large fraction of the adsorbed dye was released in a single step, the desorption efficiency in the first cycle reaching roughly 94 %. This dual control is the main practical advantage over single-responsive adsorbents, where release is often slow or incomplete [9,22].

Table 4 Comparison of the Maximum Monolayer Adsorption Capacity (q_m) of the Dual-Network Hydrogel with Other Reported Adsorbents for Basic Blue 41.

Adsorbent	q_m (mg g ⁻¹)	pH	T (°C)	Reference
Nanoporous silica (NPS)	345	7	25	Zarezadeh-Mehrizi & Badiei [5]
Zr-porous clay heterostructure	346	—	25	Al Dmour et al. [6]
Persea americana activated carbon	625	—	25	Regti et al. [3]
Activated carbon (filamentous algae)	125	9	25	Afshin et al. [4]
Bituminous shale	55	—	25	Müftüoğlu et al. [25]
PVA/bentonite hydrogel	—	—	25	Sanchez et al. [23]
Katira gum nanocomposite hydrogel	—	—	25	Jana et al. [24]
Dual-network hydrogel (this work)	384.6	8	25	This work

The gel was then carried through five successive adsorption–desorption cycles. The removal efficiency declined only gradually, and after the fifth cycle the hydrogel still retained close to 88% of its original capacity. The modest loss is most probably due to a small amount of dye that remains irreversibly bound in the deeper parts of the network, together with minor mechanical wear during repeated handling. Comparable retention has been reported for other regenerable hydrogels after five cycles [10], so the present material sits well within the useful range. The fact that the carboxylate groups can be

switched “on” and “off” by pH, and that the porosity can be opened and closed by temperature, means the same batch of adsorbent could in principle be used many times attractive both economically and from a waste-minimisation standpoint. A short comparison with previously reported BB41 adsorbents is given in Table 4, where the dual-network hydrogel compares favourably in capacity and, in particular, in ease of regeneration [5,23-25].

IV. CONCLUSION

A dual-network hydrogel responding to both pH and temperature was successfully synthesised and shown to be an effective, reusable adsorbent for Basic Blue 41. The carboxylate groups of the acrylic acid/acrylamide network supplied the binding sites for the cationic dye, while the poly(N-isopropylacrylamide) network introduced a temperature switch through its LCST. Characterisation by FTIR, XRD and FESEM confirmed the porous, amorphous, two-network structure. Adsorption was strongly favoured in mildly alkaline solution, followed pseudo-second-order kinetics and was best described by the Langmuir isotherm, with a maximum capacity of about 385 mg g⁻¹; the thermodynamic analysis showed the process to be spontaneous and exothermic. The most useful feature was the controlled release: by lowering the pH and warming the system above the LCST the captured dye could be recovered, and the gel kept close to 88 % of its capacity over five cycles. The material therefore offers a practical route to repeated dye removal with minimal waste, and similar dual-responsive designs may prove valuable for other cationic pollutants. Further work on real effluents and on long-term mechanical stability would be worthwhile.

REFERENCES

- [1]. Al-Tohamy R, Ali SS, Li F, Okasha KM, Mahmoud YA-G, Elsamahy T, et al. A critical review on the treatment of dye-containing wastewater: ecotoxicological and health concerns of textile dyes and possible remediation approaches for environmental safety. *Ecotoxicol Environ Saf.* 2022;231:113160.
- [2]. Periyasamy AP. Recent advances in the remediation of textile-dye-containing wastewater: prioritizing human health and sustainable wastewater treatment. *Sustainability.* 2024;16(2):495.
- [3]. Regti A, Lamari MR, Stiriba SE, El Haddad M. Removal of Basic Blue 41 dyes using Persea americana-activated carbon prepared by phosphoric acid action. *Int J Ind Chem.* 2017;8:187–195.
- [4]. Afshin S, Mokhtari SA, Vosoughi M, Sadeghi H, Rashtbari Y. Data of adsorption of Basic Blue 41 dye from aqueous solutions by activated carbon prepared from filamentous algae. *Data Brief.* 2018;21:1008–1013.
- [5]. Zarezadeh-Mehrizi M, Badiei A. Highly efficient removal of Basic Blue 41 with nanoporous silica. *Water Resour Ind.* 2014;5:49–57.
- [6]. Al Dmour H, Kooli F, Mohmoud A, Liu Y, Popoola SA. Al and Zr porous clay heterostructures as removal agents of Basic Blue-41 dye from an artificially polluted solution: regeneration properties and batch design. *Materials (Basel).* 2021;14(10):2528.
- [7]. Liu C, Liu H, Xiong T, Xu A, Pan B, Tang K. Graphene oxide reinforced alginate/PVA double-network hydrogels for efficient dye removal. *Polymers (Basel).* 2018;10(8):835.
- [8]. Rueda JC. Removal of methylene blue by hydrogels based on N,N-dimethylacrylamide and 2-oxazoline macromonomer. *J Polym Res.* 2020;27(9):263.
- [9]. Li Y, Ran T, Yang H, Dong Z, Shi Y. Ir-reversible on/off switching hydrogel for efficient dye capture and release. *J Environ Chem Eng.* 2023;11(3):109829.
- [10]. Hua BY, Wei HL, Hu CW, Zhang YQ, Shen YM, Li JJ. Preparation of pH/temperature-sensitive semi-interpenetrating network hydrogel adsorbents from sodium alginate via photopolymerization for removing methylene blue. *Int J Environ Sci Technol.* 2024;21(1):227–244.
- [11]. Li Y, Qu G, Zhang H, Xie L, Zhang YF. pH-responsive removal of dyes from wastewater using MXene-composited L-cysteine-grafted HEMA hydrogel: dynamics, selectivity, regeneration and mechanism. *Chem Eng Sci.* 2024
- [12]. Franco S, Buratti E, Nigro V, Bertoldo M, Ruzicka B, Angelini R. Thermal behaviour of microgels composed of interpenetrating polymer networks of poly(N-isopropylacrylamide) and poly(acrylic acid): a calorimetric study. *Polymers (Basel).* 2022;14(1):115.
- [13]. Rengifo J, Zschoche S, Voit B, Rueda JC. Synthesis and characterization of new interpenetrated hydrogels from N-isopropylacrylamide, 2-oxazoline macromonomer and acrylamide. *Eur Polym J.* 2022;177:111456.
- [14]. Lagergren S. Zur Theorie der sogenannten Adsorption gelöster Stoffe. *K Sven Vetenskapsakad Handl.* 1898;24(4):1–39.
- [15]. Ho YS, McKay G. Pseudo-second order model for sorption processes. *Process Biochem.* 1999;34(5):451–465.
- [16]. Weber WJ, Morris JC. Kinetics of adsorption on carbon from solution. *J Sanit Eng Div ASCE.* 1963;89(2):31–60.
- [17]. Langmuir I. The adsorption of gases on plane surfaces of glass, mica and platinum. *J Am Chem Soc.* 1918;40(9):1361–1403.
- [18]. Freundlich HMF. Über die Adsorption in Lösungen. *Z Phys Chem.* 1906;57:385–470.
- [19]. Temkin MI, Pyzhev V. Recent modifications to Langmuir isotherms. *Acta Physicochim URSS.* 1940;12:217–222.
- [20]. Adeyemo AA, Adeoye IO, Bello OS. Adsorption of dyes using different types of clay: a review. *Appl Water Sci.* 2017;7:543–568.
- [21]. Alharby NF, Almutairi RS, Mohamed NA. Adsorption behavior of methylene blue dye by a novel cross-linked O-CM-chitosan hydrogel in aqueous solution: kinetics, isotherm and thermodynamics. *Polymers (Basel).* 2021;13(21):3659.
- [22]. Srivastava N, Choudhury AR. Green synthesis of pH-responsive, self-assembled, novel polysaccharide composite hydrogel and its application in selective capture of cationic/anionic dyes. *Front Chem.* 2021;9:761682.

- [23]. Sanchez L, Ollier R, Alvarez VA. Sorption behavior of polyvinyl alcohol/bentonite hydrogels for dyes removal. *J Polym Res.* 2019;26:142.
- [24]. Jana S, Mondal B, Tripathy T. Efficient and selective removal of cationic organic dyes from their aqueous solutions by a nanocomposite hydrogel, katira gum-cl-poly(acrylic acid-co-N,N-dimethylacrylamide)-bentonite. *Appl Clay Sci.* 2019;173:46–64.
- [25]. Müftüoğlu AE, Karakelle B, Ergin M, Erkol AY, Yilmaz F. The removal of Basic Blue 41 dye from aqueous solutions by bituminous shale. *Adsorpt Sci Technol.* 2003;21(8):751